Anharmonic resonant Raman modes in Mg$_{0.2}$Zn$_{0.8}$O

Jesse Huso,[1] John L. Morrison,[1] Leah Bergman,[1] and Matthew D. McCluskey[2,*]

[1]*Department of Physics, University of Idaho, Moscow, Idaho 83844-0903, USA*
[2]*Department of Physics and Astronomy, Washington State University, Pullman, Washington 99164-2814, USA*
(Received 11 January 2013; published 25 March 2013)

High-order optical phonon modes in wurtzite ZnO and MgZnO nanocrystals were investigated using resonant Raman spectroscopy. The Raman modes in ZnO showed agreement with a harmonic model, consistent with prior work. MgZnO, in contrast, exhibited a large degree of anharmonic behavior. The strength of the anharmonicity increases upon application of hydrostatic pressure. These results suggest a harmonic-to-anharmonic phase transition, which could be related to the anisotropy (c/a ratio) of the crystal structure.

I. INTRODUCTION

Crystal vibrations are commonly modeled within the harmonic approximation. However, anharmonic effects influence physical phenomena such as thermal expansion,[1] phase transitions,[2] and vibrational energy transfer.[3–8] Resonant Raman spectroscopy is a technique that reveals high-order optical phonon modes, enabling one to probe the crystal potential.[9] In typical semiconductors, these modes show excellent agreement with a simple harmonic potential. In this paper, we report strongly *anharmonic* behavior in MgZnO, a wide-band-gap semiconductor alloy.

Zinc oxide (ZnO) has attracted much attention due to its uv band gap and high exciton binding energy for use in optoelectronic applications.[10–16] The Mg$_x$Zn$_{1-x}$O system has also generated interest for technological applications, particularly new light sources and detectors in the deep uv range.[17–20] However, much remains unknown about this system, with such important properties as the equation of state only being reported recently.[21]

II. EXPERIMENTAL

In the present work, ZnO and Mg$_{0.2}$Zn$_{0.8}$O nanocrystalline powders were synthesized by thermal decomposition of acetates as described by Bergman *et al.*[22] These samples, hereafter referred to as ZnO and MgZnO, were studied by resonant Raman spectroscopy using a HORIBA Jobin Yvon T64000 micro-Raman/photoluminescence (PL) system with a $\approx$1-μm spot size. The excitation source was a cw Kimmon HeCd laser operating at 325 nm (3.8 eV). Typically, PL is observed in the area of interest, which obscures high-order Raman modes. This effect is particularly pronounced for the Mg$_x$Zn$_{1-x}$O system, where strong luminescence occurs near the exciting laser line. It was shown by Huso *et al.*[23] that incorporation of small amounts of Cu^{2+} in the Mg$_x$Zn$_{1-x}$O lattice significantly reduces the band-edge PL intensity. As a consequence, the high-order Raman modes become observable and allow the study of the crystal potential. In the present work, samples were doped with $\approx$0.5 at. % Cu to suppress the PL.[24]

In resonant Raman scattering, when an incoming photon is near the energy of an electronic state of the material, phonons may be excited to produce a multiorder Raman spectrum.[25] In a simple harmonic oscillator, the energy levels are spaced equally

$$E_{m+1} - E_m = \hbar\omega, \tag{1}$$

where ω is the oscillation frequency and E_m and E_{m+1} are adjacent energy levels. For a multiorder Raman spectrum, the resonant LO Raman modes are positioned according to[26,27]

$$\omega_s^{(n)} = \omega_L - n\omega_{\mathrm{LO}}, \tag{2}$$

where $\omega_s^{(n)}$ is the frequency of the nth-order LO Raman mode, ω_L is the frequency of the incident laser photon, n is the order number, and ω_{LO} is the LO phonon frequency.

III. RESULTS

A. ZnO and MgZnO at ambient pressure

Resonant Raman spectra of ZnO and MgZnO are shown in Fig. 1. The residual PL in the MgZnO spectrum has a higher energy than that of ZnO, due to its larger band gap.[8,28] Multiple high-order Raman modes are clearly visible, up to the ninth order in ZnO and seventh order in MgZnO. Figure 2 presents a summary of the peak positions of ZnO, with resonant Raman data on ZnO reported by Scott[29] for comparison. The divergence from harmonic behavior was calculated using Eq. (2). It is possible that Cu^{2+} could affect the Raman modes. However, comparing our results with those of Scott suggests that the presence of Cu^{2+} has no significant impact on the harmonic behavior of the Raman modes, which is the focus of this paper. Both data sets follow the harmonic model closely and show little deviation even for high orders. The minor difference in the absolute Raman frequencies may be due to differences in sample quality.

In contrast, Fig. 3 presents a plot of the peak positions of the MgZnO Raman spectrum, along with the expected harmonic frequencies [Eq. (2)]. The MgZnO data show a large divergence from the harmonic model. In attempt to quantify the anharmonicity, we may analyze the results in terms of an alternative to the simple harmonic oscillator, specifically the Morse potential,[30,31]

$$V(r) = D_e[e^{-\beta r} - 1]^2, \tag{3}$$

where D_e is the binding energy and β is the Morse parameter. The energy eigenvalues for this potential may be expressed as

$$E_n = \hbar\omega_e \left(n + \tfrac{1}{2}\right)\left[1 - \chi_e\left(n + \tfrac{1}{2}\right)\right], \tag{4}$$
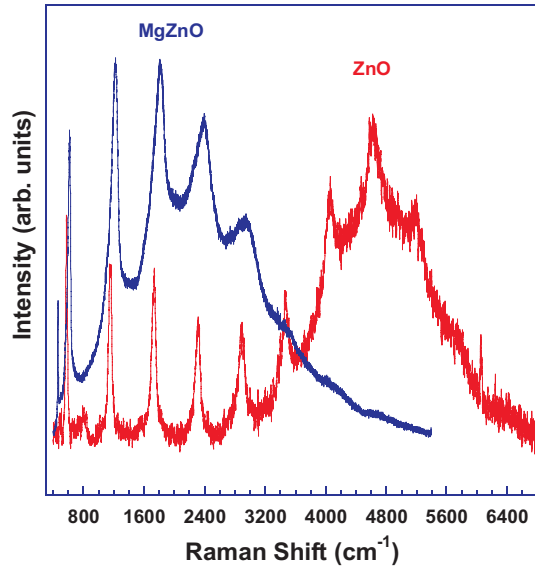
FIG. 1. (Color online) Resonant Raman spectra of ZnO and MgZnO at room temperature, showing high-order LO modes. The shift in the PL is due to the larger band gap of MgZnO as compared with ZnO.

where the coefficients χ_e and ω_e are

$$\omega_e = \beta\,(2D_e/\mu)$$
$$\chi_e\omega_e = \hbar\beta^2/2\mu \tag{5}$$

and μ is the reduced mass. Note that the energy levels of the Morse potential become more closely spaced with increasing n.

The observed nth-order Raman mode is the difference between the nth excited state E_n and the ground state E_0. The
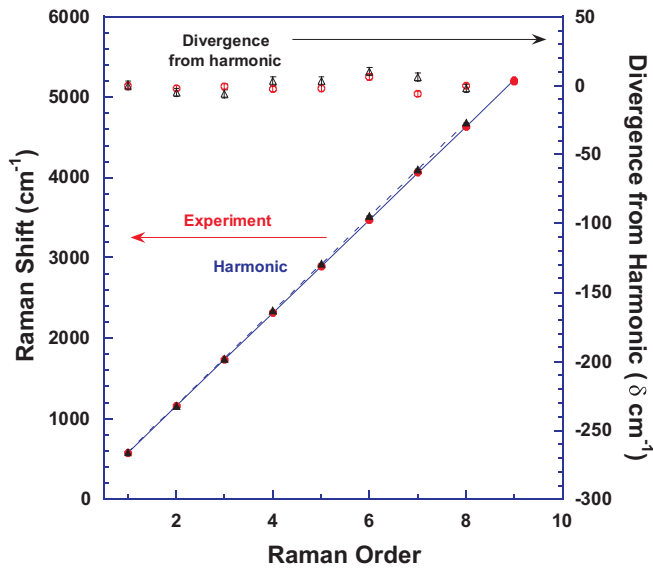
FIG. 2. (Color online) Resonant Raman modes for ZnO (red, circles), with data from Scott (Ref. 29; black, triangles) for comparison. The left axis denotes the frequency of the Raman modes (filled symbols). Fits to the harmonic approximation [Eq. (2)] are shown by the solid and dashed lines. The deviation of the data from harmonic behavior is shown on the right axis (open symbols).
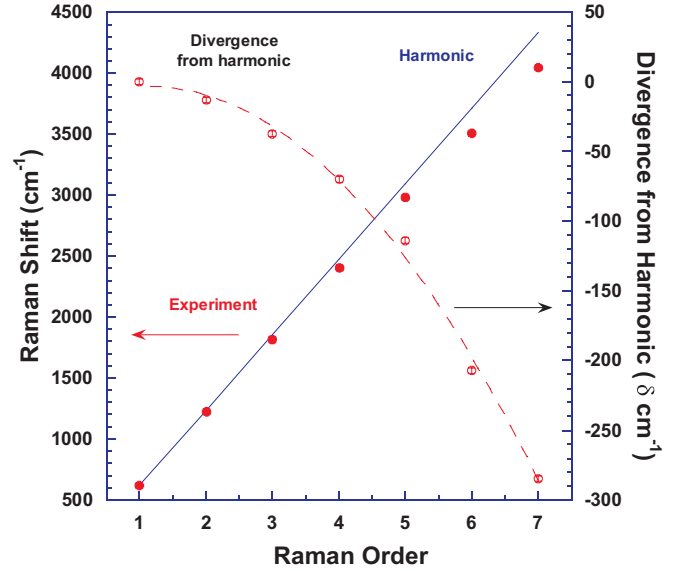
FIG. 3. (Color online) Resonant Raman modes for MgZnO. The left axis denotes the position of the Raman modes (filled circles). A fit to the harmonic approximation is shown by the solid line. The deviation of the data from harmonic behavior is shown on the right axis (open circles). The dashed curve is a fit to the deviation, using the Morse potential [Eq. (6)].

Raman modes will differ if they arise from a Morse potential as opposed to a harmonic potential. One may calculate the expected difference in the models for a given mode as

$$\Delta_{n0}^M - \Delta_{n0}^H = \hbar n(\omega_e - \omega_e\chi_e - \omega) - \hbar\omega_e\chi_e n^2, \tag{6}$$

where $\Delta_{n0} = E_n - E_0$ denotes the difference between the nth excited state and the ground state, M and H denote the Morse and harmonic potentials, respectively, and ω is the frequency of the simple harmonic oscillator. The dashed curve in Fig. 3 shows the divergence from harmonic, calculated from Eq. (6), with fitted parameters $\omega_e = 633(3)$ cm^{-1} and $\chi_e = 0.011(1)$.

B. MgZnO under pressure

To probe the anharmonicity of MgZnO further, the material was studied under hydrostatic pressure in a diamond anvil cell (DAC). A D'Anvils DAC was used with 0.6-mm culets, stainless steel gaskets, and a 4:1 methanol:ethanol mixture as the pressure medium. The pressure was measured by using the shift of the TO Raman mode of cubic boron nitride as calibrated by Datchi and Canny.[32] In order to ensure stable pressure conditions, upon compression, the cell was allowed to rest for 20 min, whereupon the pressure was measured. After data were collected, the pressure was measured again. If the initial and final pressure measurements disagreed, the obtained data were not used, and the described data collection process was repeated until consistent readings were obtained.[33]

Representative resonant Raman spectra of MgZnO, for the first three orders of LO phonons, are presented in Fig. 4 for several pressures. For a harmonic potential, the frequency shift versus pressure should be proportional to the order n [Eq. (2)]. Figure 5 presents a summary of the Raman data as a function of pressure along with the expected behavior from a harmonic system, where the trends are linear fits to the
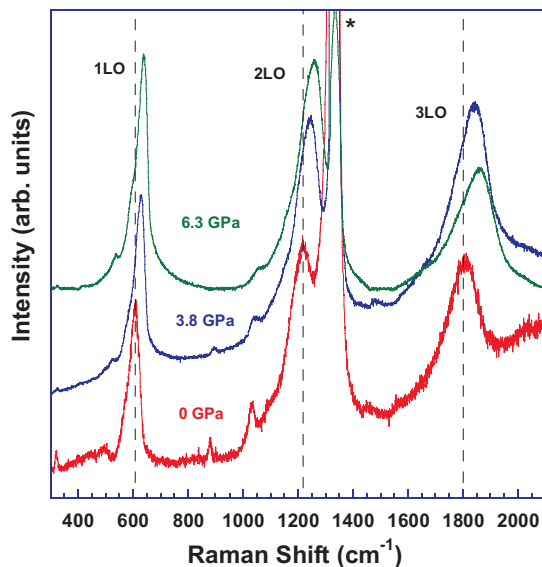
FIG. 4. (Color online) Room-temperature resonant Raman spectra of MgZnO for several pressures. The Raman modes show a shift with applied pressure. The peak marked with * is from the diamonds.

data. The divergence from harmonic behavior becomes more pronounced with applied pressure.

By fitting the mode frequencies to the Morse potential [Eq. (4)], we obtained χ_e and ω_e for each pressure. Plotting these calculated coefficients shows the behavior of the potential as a function of pressure (Fig. 6). The coefficients were
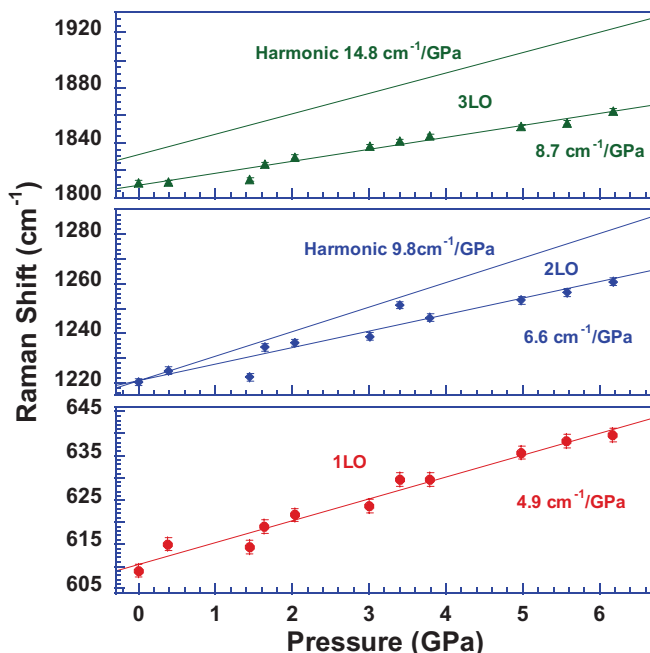
FIG. 5. (Color online) Raman shift as a function of pressure for the MgZnO. The observed slopes diverge from the behavior expected for a harmonic system. This anharmonicity becomes more pronounced with applied pressure.
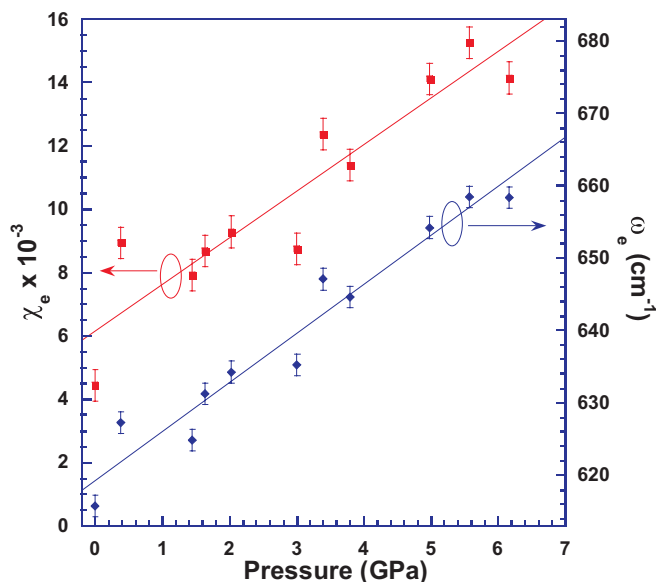
FIG. 6. (Color online) Morse potential parameters for MgZnO as a function of pressure. The results indicate that the anharmonicity increases with applied pressure.

found to shift linearly with pressure

$$\chi_e(P) = 6.1(0.7) \times 10^{-3} + 1.5(0.2) \times 10^{-3} P$$
$$\omega_e(P) = 619(2) + 6.8(0.6)P, \tag{7}$$

where P is the pressure in gigapascals and ω_e is in wave numbers cm^{-1}. The results indicate that the crystal potential of MgZnO undergoes significant increase in anharmonicity with applied pressure.[34]

IV. CONCLUSIONS

The observation of such a large degree of anharmonicity in LO phonons for MgZnO stands in contrast to prior work on other crystals. For example, Li et $al.$[35] performed resonant Raman scattering experiments as a function of pressure on Zn$_x$Cd$_{1-x}$Se, and their results indicate no anharmonicity. Raman modes in other II-VI semiconductors are also well described by the simple harmonic model.[26,29,36] Choi and Yu[37] found that the resonant modes in CdS followed a harmonic model at ambient pressure. Under pressure, high-order modes showed small deviations from the harmonic model. For the third-order LO mode, the harmonic approximation yielded a pressure coefficient ≈7% too high, as compared with 70% in the present work (Fig. 5).

Why does MgZnO exhibit such large anharmonicity? While it is clear that the presence of Mg in the lattice is correlated with anharmonicity, the actual mechanisms for this transformation are currently unknown. It is conceivable that the ionic nature of the MgO bond is responsible for the change in the harmonic behavior observed between ZnO and MgZnO. The increase in ionicity with Mg content could cause an increase in anharmonicity. However, Serrano et $al.$[38] reported that the effective transverse charge of ZnO decreases with pressure, as is the case in most semiconductors.[39] This suggests that the

ionicity of ZnO or MgZnO decreases with pressure, opposite to the effect of Mg alloying.

A further possibility is that our results could be related to the c/a ratio for hexagonal crystals. The unit cell volume for MgZnO and ZnO are nearly the same[28] and the c/a ratio of $Mg_x Zn_{1-x}O$ decreases with increasing Mg content[28] and hydrostatic pressure.[21,40] For $Mg_{0.2}Zn_{0.8}O$ at ambient pressure, $c/a \approx 1.59$.[21] Other wurtzite II-VI semiconductors have higher c/a ratios (CdS: 1.62; CdSe: 1.63; ZnO: 1.61; ZnS: 1.64), which are closer to the ideal tetrahedral bonding value of 1.63.[41] These observations suggest that there is a critical c/a value for a "harmonic-to-anharmonic" phase transition. When this ratio drops below ≈ 1.6 in MgZnO, anisotropic distortion causes the crystal potential to become anharmonic. Interestingly, Venkateswaran *et al.*[42] mention a change in phonon behavior in CdS at around 2.5 GPa: below this pressure, the phonon behavior is close to harmonic, while above 2.7 GPa, their material became slightly anharmonic.

The harmonic pressure coefficient was about 6% too high for the 2LO mode, similar to the findings of Choi and Yu.[37] This lends support to the hypothesis that there may be a critical c/a ratio for the onset of anharmonic behavior.

To reiterate, the fundamental cause of the onset of anharmonicity is currently unknown. Further experiments to elucidate the underlying cause of this unusual anharmonic behavior, particularly as a function of Mg content, are currently underway.

*mattmcc@wsu.edu

[1] C. Kittel, *Introduction to Solid State Physics* (Wiley, Hoboken, NJ, 2005).

[2] N. Sai and D. Vanderbilt, Phys. Rev. B **62**, 13942 (2000).

[3] G. Lüpke, N. H. Tolk, and L. C. Feldman, J. Appl. Phys. **93**, 2317 (2003).

[4] L. Hsu, M. D. McCluskey, and J. L. Lindström, Phys. Rev. Lett. **90**, 095505 (2003).

[5] M. D. McCluskey, Phys. Rev. Lett. **102**, 135502 (2009).

[6] R. Cuscó, N. Domènech-Amador, L. Artús, K. Wang, T. Yamaguchi, and Y. Nanishi, J. Appl. Phys. **112**, 053528 (2012).

[7] S. K. Estreicher and D. West, Nucl. Instrum. Methods Phys. Res., Sect. B **253**, 196 (2006).

[8] G. Davies, J. Phys.: Condens. Matter **22**, 505801 (2010).

[9] L. Bergman, M. Dutta, and R. J. Nemanich, in *Raman Scattering in Materials Science*, 1st ed., edited by W. H. Weber and R. Merlin (Springer, Berlin, 2000), p. 274.

[10] M. Kawasaki, A. Ohtomo, I. Ohkubo, H. Koinuma, Z. K. Tang, P. Yu, G. K. L. Wong, B. P. Zhang, and Y. Segawa, Mater. Sci. Eng. B **56**, 239 (1998).

[11] Y. Chen, D. M. Bagnall, H. Koh, K. Park, K. Hiraga, Z. Zhu, and T. Yao, J. Appl. Phys. **84**, 3912 (1998).

[12] S. Yang, J. Gong, and Y. Deng, J. Mater. Chem. **22**, 13899 (2012).

[13] Y.-J. Lin, T.-H. Su, J.-C. Lin, and Y.-C. Su, Synth. Met. **162**, 406 (2012).

[14] P. F. Carcia, R. S. McLean, and M. H. Reilly, Appl. Phys. Lett. **88**, 123509 (2006).

[15] D. C. Olson, J. Piris, R. T. Collins, S. E. Shaheen, and D. S. Ginley, Thin Solid Films **496**, 26 (2006).

[16] M. S. White, D. C. Olson, S. E. Shaheen, N. Kopidakis, and D. S. Ginley, Appl. Phys. Lett. **89**, 143517 (2006).

[17] L. K. Wang, Z. G. Ju, J. Y. Zhang, J. Zheng, D. Z. Shen, B. Yao, D. X. Zhao, Z. Z. Zhang, B. H. Li, and C. X. Shan, Appl. Phys. Lett. **95**, 131113 (2009).

[18] Z. G. Ju, C. X. Shan, D. Y. Jiang, J. Y. Zhang, B. Yao, D. X. Zhao, D. Z. Shen, and X. W. Fan, Appl. Phys. Lett. **93**, 173505 (2008).

[19] D. Y. Jiang, C. X. Shan, J. Y. Zhang, Y. M. Lu, B. Yao, D. X. Zhao, Z. Z. Zhang, D. Z. Shen, and C. L. Yang, J. Phys. D **42**, 025106 (2009).

[20] Z. L. Liu, Z. X. Mei, T. C. Zhang, Y. P. Liu, Y. Guo, X. L. Du, A. Hallen, J. J. Zhu, and A. Y. Kuznetsov, J. Cryst. Growth **311**, 4356 (2009).

[21] G. J. Hanna, S. T. Teklemichael, M. D. McCluskey, L. Bergman, and J. Huso, J. Appl. Phys. **110**, 073511 (2011).

[22] L. Bergman, J. L. Morrison, X.-B. Chen, J. Huso, and H. Hoeck, Appl. Phys. Lett. **88**, 023103 (2006).

[23] J. Huso, J. L. Morrison, J. Mitchell, E. Casey, H. Hoeck, C. Walker, L. Bergman, W. M. Hlaing Oo, and M. D. McCluskey, Appl. Phys. Lett. **94**, 061919 (2009).

[24] The small mass difference between Cu and Zn, on the order of 2.8% and the low concentrations of Cu, suggest that there would be little modification to the phonon modes by the presence of Cu in the lattice.

[25] P. Y. Yu and M. Cardona, *Fundamentals of Semiconductors: Physics and Materials Properties* (Springer, Berlin, 1996).

[26] J. F. Scott, T. C. Damen, W. T. Silfvast, R. C. C. Leite, and L. E. Cheesman, Opt. Commun. **1**, 397 (1970).

[27] J. F. Kong, W. Z. Shen, Y. W. Zhang, C. Yang, and X. M. Li, Appl. Phys. Lett. **92**, 191910 (2008).

[28] A. Ohtomo, M. Kawasaki, T. Koida, K. Masubuchi, H. Koinuma, Y. Sakurai, Y. Yoshida, T. Yasuda, and Y. Segawa, Appl. Phys. Lett. **72**, 2466 (1998).

[29] J. F. Scott, Phys. Rev. B **2**, 1209 (1970).

[30] M. D. McCluskey, J. Appl. Phys. **87**, 3593 (2000).

[31] I. N. Levine, *Physical Chemistry* (McGraw-Hill, Boston, 2002).

[32] F. Datchi and B. Canny, Phys. Rev. B **69**, 144106 (2004).

[33] J. Huso, J. L. Morrison, H. Hoeck, X.-B. Chen, L. Bergman, S. J. Jokela, M. D. McCluskey, and T. Zheleva, Appl. Phys. Lett. **89**, 171909 (2006).

[34] The MgZnO sample loaded in the DAC had a slightly lower Mg concentration than the sample measured at ambient conditions. The DAC sample had a first-order Raman peak at $609\,cm^{-1}$, as compared with $619\,cm^{-1}$ for the other sample.

[35]W. S. Li, Z. X. Shen, D. Z. Shen, and X. W. Fan, J. Appl. Phys. **84**, 5198 (1998).

[36]R. C. C. Leite, J. F. Scott, and T. C. Damen, Phys. Rev. Lett. **22**, 780 (1969).

[37]I. H. Choi and P. Y. Yu, Phys. Status Solidi B **242**, 2813 (2005).

[38]J. Serrano, A. H. Romero, F. J. Manjón, R. Lauck, M. Cardona, and A. Rubio, Phys. Rev. B **69**, 094306 (2004).

[39]E. Anastassakis and M. Cardona, in *High Pressure in Semiconductor Physics. II*, edited by T. Suski and W. Paul (Academic Press, New York, 1998), p. 117.

[40]K. K. Zhuravlev, W. M. Hlaing Oo, M. D. McCluskey, J. Huso, J. L. Morrison, and L. Bergman, J. Appl. Phys. **106**, 013511 (2009).

[41]M. D. McCluskey and E. E. Haller, *Dopants and Defects in Semiconductors* (Taylor & Francis, Boca Raton, FL, 2012).

[42]U. Venkateswaran, M. Chandrasekhar, and H. R. Chandrasekhar, Phys. Rev. B **30**, 3316 (1984).